SAE International™

Rollover Crash Test Results: Steer-Induced Rollovers

2011-01-1114
Published
04/12/2011

Don C. Stevens, Stephen Arndt and Leda Wayne
Safety Engineering and Forensic Analysis

Mark Arndt
Transportation Safety Technologies, Inc.

Robert Anderson
Biomechanics Analysis

Joseph Manning
Collision Dynamics, LLC

Russell Anderson
Collision Analysis & Research

doi:10.4271/2011-01-1114

ABSTRACT

A series of rollover tests was conducted in a real-world environment in which a vehicle was driven or towed to highway speed then steered to induce a rollover. This research presents analysis of the rollover phase of five tests. In each test, the steering maneuver was initiated on-pavement, and the rollover was caused by tire-to-ground interaction. Tests included vehicles that tripped both on-pavement and on soil. Four tests ended with the vehicle at rest off-road, and one ended with the vehicle remaining on the pavement. A programmable remote control radio was used to steer the vehicles through a double-step steer maneuver to result in a rollover. The test vehicles were instrumented and data was collected during each test, including steering, suspension motion, rotational rates, and accelerations. A Global Positioning System (GPS) speed sensor (VBOX III manufactured by Racelogic) was used to monitor the vehicle speed. Data from all tests is presented in the Appendix . Each test was recorded from multiple perspectives using real-time and high-speed video cameras. The electronic data acquisition was synchronized with the vehicle's roadway position and with each video camera using flashbulbs and a chalk gun. The crash site evidence was documented through surveying and photography. The scratch patterns and crush damage to each test vehicle were studied and photographed. Each test was analyzed in detail, including calculation of the speed over the ground throughout the rollover, drag factors, and rollover distances. The calculated speed at trip was compared to the output of the VBOX speed sensor. Based on this comparison, validation testing of the VBOX was conducted and a correction formula for VBOX trip speed is proposed.

INTRODUCTION

The majority of rollover testing to date has been conducted in a controlled environment using a test device to initiate the rollover. Recent publications have shown that, compared to dolly rollover tests, steer-induced rollovers in a real-world setting provide a more realistic representation of an actual rollover event. This paper presents the results and analysis of five such rollover tests conducted between July 2009 and June 2010.

PRIOR PUBLICATION OF STEER-INDUCED ROLLOVER TESTS

Steer-induced rollovers are also referred to in the literature as "steering controller tests" (Yaek [1]) and "tests on an actual highway" (Asay and Woolley [2]). Though its stated aim was to present tools for recreating rollover crashes, Larson [3] demonstrated the feasibility of a naturally-occurring rollover test as a research tool for developing, evaluating, and validating methods for the reconstruction of rollover crashes. In 2007 Wilson, Gilbert, and Godrick [4] presented results of two staged crashes in which rollovers on a ground-based grid were induced by steering alone. Post-test analyses of the videotaped rollovers yielded calculated rollover deceleration rates and scaled drawings depicting vehicle motions and surface marks.

Asay and Woolley [2] published the first of two papers in 2009 that described a method for testing on an actual highway. The method used a large truck to tow an instrumented vehicle with a programmable steering controller on a two-lane highway. The towed vehicle was released from the truck and then steered in a manner that resulted in an off-road path and subsequent rollover. Limitations in the speed measuring device required the trip speed to be extrapolated over the entire distance from the location that each vehicle left the paved road surface to the trip point. Despite limitations, this paper represented a breakthrough in steer-induced, real-world rollover testing.

Asay and Woolley's 2010 paper [5] reported on six rollover tests of sport utility vehicles on an actual highway, offering further improvement in test instrumentation and test control. Vehicle speed was measured with a VBOX GPS sensor. The trip speed for three of the tests was determined by extrapolation or interpolation of the recorded speed. Substantial insight into the interpretation of the instrumented vehicles' recorded response was presented.

ROLLOVER PHASES

The study of rollover crashes in distinct phases is at least as old as the often-cited study published by Hight, Siegel, and Nahum [6] at the 1972 Stapp Car Crash Conference. Hight and his co-authors describe rollover causation as a sequence of three phases that starts with driving, followed by tripping and rollover. Phases of rollover causation were later discussed by Orlowski *et al.* [7] which included discussion of pre-trip tire marks, tripping, and the airborne phase.

A clear description of the phases of a rollover sequence was provided by Martinez and Schlueter [8] in which they describe a pre-trip phase, trip phase, and post-trip phase. Meyer *et al.* [9] describe three rollover phases, adopting and refining Martinez's definition for the start of the tripping phase. They stated: "Rollovers are generally considered in three distinct stages. The pre-trip phase; the trip phase; and the post-trip or rollover phase. The pre-trip phase is typically considered to begin at loss of vehicle control and end at the point where wheel lift occurs. The trip phase covers the portion of the accident wherein the trailing wheels lift, or leave the surface of the roadway and the vehicle begins to rollover. The rollover phase, then, can be considered to be the rolling or tumbling portion of the accident before the vehicle comes to rest."

ROLL PHASE

Historically, rollover testing utilized a "208 Rollover Dolly" and the method described in the SAE J2114 recommended practice. Over time, numerous test methods for examining the rollover phase have been used, including reconstruction analysis (with and without a video recorder), dolly rollover tests (on asphalt and on soil), curb- and soil-induced rollover tests, modified dolly rollover tests, NHTSA's Rollover Test Device (RTD), Controlled Rollover Impact System (CRIS) tests, and steer-induced rollover tests.

The roll phase begins at the point of four-wheel lift. In crash reconstruction, this beginning point was assumed to be the end of tire marking and was described by Orlowski [7]; "The beginning of the airborne rollover trajectory and path can be defined as that point along the path at which the vehicle center of gravity is over the tire or wheel contact with the ground surface. Thus, any rotation of the vehicle beyond this point will result in a rollover, as opposed to the vehicle returning (falling back) onto its wheels. This point is approximately at the ending of the tire marks. The beginning of the tripping process will occur earlier." The rollover phase ends at the vehicle point of rest.

ROLLOVER DRAG FACTOR

Calculation of a vehicle's speed at trip commonly utilizes a drag factor over the roll distance. Hight, Siegel, and Nahum performed reconstruction analysis consistent with available knowledge and methods in use prior to their 1972 paper. The often-cited 0.4-0.65g drag factor range originates from this source and represents 60 percent of the vehicles that rolled on level ground. Orlowski [7] reported on 41 dolly rollover crash tests where the trip speed and rollover distance were measured from the launch point. The average deceleration in these tests was reported to be 0.42g with a range of 0.36-0.61g. Yaek [1] summarized rollover test drag factors, including 51 rollover tests using the 208 Dolly, many of which were previously reported by Orlowski. Yaek also reported ten RTD tests with more than two quarter rolls, seven RTD tests with two quarter rolls or less, three steer-induced tests, two curb tests, two soil tests, and eight curb trip tests with a 208 Dolly at 0°. Yaek summarized the rollover test decelerations data (drag factors) as having a range of 0.32-0.65g with an average of 0.44g.

Luepke *et al.* [10] reported on five dolly rollovers conducted on dirt. The tests used the 208 Dolly with the leading edge of the tires resting against a four-inch tall steel plate. Luepke reported the roll distance and associated drag factor from the launch point (0.50 - 0.58g with a 0.53g average) and from the point of first ground contact (0.50-0.61g with a 0.55g average). In a follow-up paper, Carter *et al.* [11] analyzed the first two of Luepke's rollovers and reported drag factors from the point of first contact (0.55g) and from the end of first contact tire marks (0.48g and 0.53g). They discussed drag factor from a break-over angle which they define as the "roll angle where the CG passes beyond a vertical projected from the point of contact at the onside tires." In a dolly rollover the break-over angle was described as occurring sometime between the beginning and end of tire marking.

Carter provided an extended technical discussion on the physics of rollovers observing that during airborne phases angular and translational velocities were constant. Carter also stated that a multiphase approach to reconstructing rollover crashes was suggested by his results. A variable deceleration rate approach to rollover reconstruction in which the drag factor linearly decreases was presented by Rose and Beauchamp [12]. The approach was described as reducing error in reconstructed translational and angular velocity time-histories.

Anderson *et al.* [13] reconstructed an actual highway-speed rollover crash event involving a sport utility vehicle (SUV). Using a single video of the accident, recorded by a law enforcement vehicle, along with data from inspections of both the crash site and the accident vehicle, they analyzed the rollover sequence. The vehicle rolled six times over asphalt and soil surfaces, coming to rest on the roadway shoulder. Anderson reported an average drag factor over the 250 foot roll distance of 0.43g.

The accuracy of the drag factor derived from controlled rollover testing is dependent on the ability to measure both the rollover distance and the speed at the point of trip. The rollover distance is typically determined by surveying the post-test evidence starting from the point of trip (last evidence of tire marks), continuing along the roll path (ground strikes and debris), and ending at the final rest position. The speed at the point of trip can be determined by a variety of methods, including radar, integration of measured accelerations, and video analysis. Additionally, the use of GPS speed sensors for measurement of speed during a rollover test has gained popularity in recent years.

GPS SPEED SENSOR

The Racelogic VBOX instrument reports vehicle speed in the xy-plane. VBOX speed data is based on accurately measuring the Doppler shift of the radio signal from the GPS satellites. The more satellites from which the VBOX antenna can receive signals, the more accurate the reported speed becomes. This requires that the antenna be placed in a position on the test vehicle so that it has an unobstructed view of the sky through as much of the rollover event as possible. The logical placement of the antenna is the roof of the test vehicle. This provides a direct view to the maximum number of GPS satellites for the longest period of time during the rollover event.

METHODOLOGY

TEST SETUP

This series of rollover tests was conducted with four Sport Utility Vehicles (SUV's) and one minivan. A summary of vehicle and test information can be found in Table 1, and photographs of each vehicle can be found in the Appendix. The test methodology was developed and proven during Test 0 and refined based on that experience for the subsequent tests. Four tests in the study were performed at the Southwestern International Raceway in Tucson, Arizona, and one was done at Luke Air Force Base in Glendale, Arizona. The recorded and corrected trip speeds for each test are reported in the Results section of this paper.

Table 1. Vehicle and test information.

Test No.	Date	Vehicle		Test Weight (lbs)	Driven/ Towed
0	7/10/2009	1989	Ford Aerostar XL 4x2	4180	Driven
1	12/1/2009	2001	Chevrolet Blazer 2DR 4x2	4485	Driven
2	3/10/2010	2002	Ford Explorer Sport 4x2	4825	Towed
3	6/2/2010	1997	Ford Explorer Sport 4x4	5025	Towed
4	6/30/2010	1995	Nissan Pathfinder LE 4x4	4476	Driven

The vehicles were accelerated to speeds in the range of 50-70 mph and then subjected to a two-step steer input to initiate the rollover. The steering was performed using a remote control steering and braking system (Figure 1) that was designed for this research. Three of the vehicles were driven remotely under their own power, and the other two vehicle were towed to speed and released using a pneumatic release mechanism mounted on the front bumper of the test vehicle as shown in Figure 2. Data acquisition was initiated by remote control shortly before the first steer input.

The rollover surface at the speedway varied for each test and consisted of asphalt, desert soil, or both. The measured drag factor of the asphalt surface with P-metric tires was 0.68g. For two of the speedway tests, the rollover sequence initiated on the asphalt then continued off the pavement and onto the desert soil. In order to suppress dust during Test 4, a water truck was used to dampen the soil approximately one hour prior to the test. The test at Luke AFB was conducted on a concrete surface where the measured drag factor averaged 0.73g.

Figure 1. Remote-controlled steering and braking system.

Figure 2. Towing and pneumatic release system for Test 2.

Panning, high-definition cameras were manned from positions around the test site, and unmanned standard-definition cameras were stationed directly along the anticipated roll path. For Test 1 through Test 4, a Phantom Miro 1 high-speed camera was manned from an elevated position off to the side of the roll path. This camera, which can capture up to 500 frames per second for 7 seconds, was set to capture the events at 250 fps to allow for up to 14 seconds of recording time. For Test 0, the high speed camera used was a Casio EX-F1 filming at 300 fps.

VEHICLE PREPARATION

A triaxial accelerometer, comprised of IC Sensor (ICS) model 3031 uniaxial accelerometers with a range of ±100g on each axis, was mounted at the vehicle's approximate static center of gravity (CG) along with a triaxial Diversified Technical System Angular Rate Sensor (DTS ARS-8k), which has ± 8000°/sec range with a 0-300 Hz response (see Figure 3). Celesco SP1 linear displacement transducers (string potentiometers) with a 50 in range were used to measure the suspension travel at each wheel location and the steering input. The string potentiometers were not used on the wheels for the first test, Test 0.

The vehicle's speed was monitored and recorded using a GPS speed sensor which reports speed at 100 Hz accurate to ± 0.06 mph using the Doppler shift of GPS satellite signals. The Racelogic VBOXIII GPS speed sensor was used in Test 1 and upgraded to a VBOXIIIi with Inertial Measurement Unit (IMU) integration for Tests 2, 3, and 4. The IMU measures triaxial acceleration in the ±2g range and triaxial rotational rate in the ± 150°/sec range. All other accelerometer, rotational rate, and linear displacement transducer data was collected at 10 kHz using two rack-mounted DTS TDAS Pro signal input modules, each of which has a 16-bit resolution.

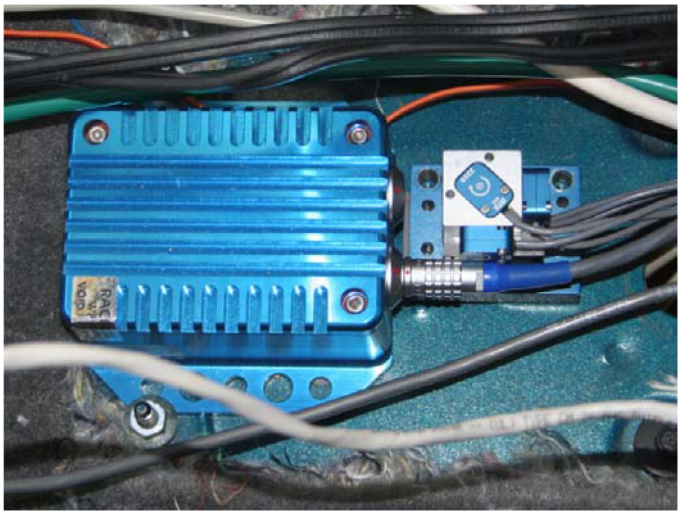

Figure 3. Accelerometer and IMU installation for Test 2.

In the test reference frame, the positive axis orientations were defined as X axis forward, Y axis to the right, and Z axis downward, in accordance with SAE J211 Recommended Practice.

Each vehicle was outfitted with a two-shot chalk gun and two flashbulbs in order to provide synchronization between the video, ground evidence and on-board data collection. The

first charge from a chalk gun and one of the bulbs were fired simultaneously with the initiation of data collection (time-zero). The secondary chalk gun load and flashbulb fired approximately 1.25 seconds later in case any camera was unable to record the primary synchronization flash.

In Test 1 through Test 4, a water dummy was placed in each of the four primary seating locations. To reduce the potential for damage to electrical instrumentation, each water dummy was filled with salt to a weight of 178 lbs. The dummies were seat belted and then anchored with additional tie-down straps to protect the interior test instruments as shown in Figure 4. In Test 0, ballast was provided via 40-lb bags of salt. The amount of ballast was 180 lbs. in each rear outboard seat position.

Figure 4. Salt-filled dummies in vehicle seating positions for Test 4.

Prior to testing, each of the side and rear glass panels on the vehicles was painted with a different color spray paint to assist in correlating glass fields on the ground with their original positions on the vehicle. Targets were painted on the exterior of the vehicle to facilitate tracking in the video footage. Additionally, one-half of each tire and wheel was painted white to improve the visibility of the wheel rotation in the videos. The vehicles were photographed before and after each test with a calibrated camera and photogrammetry targets on the exterior of the vehicle in order to facilitate three-dimensional (3D) photogrammetric modeling of the vehicles and measurement of the post-crash damage, if necessary.

CRASH SITE DOCUMENTATION

After each rollover test, the crash site was thoroughly documented using the same techniques the authors apply to accident investigations. Each site was extensively photographed, then a laser total station surveying instrument was used to measure the 3D position of the crash site geometry and all evidence of the vehicle's path before and after the overturn. The crash site measurements included the following:

- All tire marks created by the vehicle leading to the point of overturn.
- The position of each ground impact mark.
- The location of vehicle debris.
- The perimeter of each field of fractured window glass.
- The vehicle rest position.
- Reference marks created by the chalk gun.
- Video camera locations.
- Locations of permanent reference points for correlation of aerial photography.

TEST VEHICLE DOCUMENTATION

Following each test, the accident vehicle was fully inspected to document the rollover evidence. The scratch marks were studied in conjunction with the video coverage of the test and the impact marks along the roll path to determine the sequence of each scratch set. The scratches from each revolution during the overturn were tagged with different colors of masking tape. The scratch sets were then added to a scaled 3D CAD model of each vehicle.

ROLLOVER RECONSTRUCTION

Each rollover test was reconstructed from the collected data in a manner similar to the analysis of a real-world accident. The survey data was used to create a scaled drawing of the test site and all evidence of the rollover. A custom aerial photograph of each test site was correlated to the survey data. The 3D model of the test vehicle was aligned with the measured tire marks at multiple positions leading to overturn to determine the change in sideslip angle along the path. The impact marks along the rollover path were matched to the damage and scratch patterns found on the accident vehicle. The video coverage of the crash and the documented vehicle scratch patterns were used to determine the 3D orientation of the vehicle at each ground impact and at the completion of each rollover revolution. The 3D model of the test vehicle and scratch patterns was then placed on the scene diagram and aligned with each of the reconstructed positions.

ROLLOVER PHASE DURATION

In this research, the roll phase of each test was defined to begin at the point of four-wheel lift (trip point) and to end at the point of rest. The time of trip was identified from the accelerometer data as the instant when the measured accelerations dropped to zero. This position was found to

coincide with the termination of the tire marks and was confirmed by the multi-angle video coverage.

As each vehicle completed its final quarter turn in the rollover and stopped sliding, it tended to roll slightly past its final rest orientation before reversing roll direction and settling to rest. The time when the vehicle was determined to have reached its rest position was identified as the moment when the total roll angle first reached the final roll angle. The additional time required for each vehicle to settle after reaching its rest position was excluded when measuring the duration of the event.

OVER-THE-GROUND SPEED CALCULATION

The over-the-ground speed (OGS) is the rate of change in the vehicle's position in the plane of the roadway. This quantity cannot be measured directly using the GPS sensor after the rollover begins. Because the speed is a measure of the distance traveled in a unit of time, the OGS can be calculated between discrete positions along the roll path when the time elapsed while moving between successive positions is known.

The first component of the OGS calculation, the distance between ground contacts, was determined by a detailed inspection and measurement of the test site after each rollover. At the trip point, when all four tires left the ground, the termination point of each tire mark was clearly visible. Each time a vehicle contacted the ground during the rollover phase of a test, evidence of the impact was left behind at that location, including disturbed soil, pavement scrapes, paint transfers, vehicle debris, and more. The 3D position of the ground evidence was precisely measured using a laser total station.

The position of the vehicle at time-zero (start of data acquisition and firing of the first synchronization flash) was marked on the roadway by the chalk gun. The position of distinct imprint made by the chalk load was measured with the surveying instrument. In this way, the position of the vehicle at the moment of the video synchronization flash is known relative to the ground contact evidence.

A rollover diagram was created for each test by correlating the aerial photography of each site with the measured ground evidence. The location of the vehicle CG relative to the ground evidence was determined by placing a scaled 3D model of each test vehicle on the diagram at each distinct ground contact, with the model in the same orientation as the test vehicle at the moment of the impact. The distance that the vehicle's CG traveled between distinct impacts along the roll path was measured from the resulting diagram.

The second quantity needed for the OGS calculation, the time elapsed between ground contacts, was determined from the onboard instrumentation. Throughout the tests, the accelerations at the vehicle's CG resulting from each ground contact were recorded by accelerometers. The onset time and duration of each impact were read directly from the acceleration data. The instrumentation data was synchronized to the high-speed and real-time video coverage of each rollover using a flashbulb that fired at time-zero in the data. This synchronization made it possible to determine the orientation of the vehicle at each ground impact from the video and the precise timing of the contact from the corresponding acceleration pulse.

The average OGS of a test vehicle's CG during a given segment of the rollover (between the distinct impact positions) is calculated from the distance the CG moves during the segment divided by the time elapsed as the vehicle traverses the distance. The OGS for the test vehicles was calculated for each segment and then plotted for the entire roll event.

One segment of the OGS analysis of particular interest is from the trip point, at the termination of the tire marks, to the point of first ground contact. In the absence of ground forces during this airborne segment, the speed will remain essentially constant. Therefore, the vehicle's trip speed is equal to the OGS calculated for the segment from trip to first contact.

The average drag factor (μ) for each test was calculated from the OGS at trip and the total rollover distance (d). The formula for drag factor is shown in Equation 1.

$$\mu = \frac{OGS^2}{2*d*g} \tag{1}$$

VERIFICATION OF GPS SENSOR SPEED OUTPUT

The speed reported by the GPS sensor is the speed of its antenna in the xy-plane. This speed will coincide with that of the vehicle's CG whenever the antenna is not moving relative to the CG. As the vehicle approaches the trip point of a rollover test, the speed of the roof-mounted antenna will exceed that of the CG as a significant roll velocity (*p*) develops and the roof rotates to a position ahead of the rest of the vehicle.

A simple test was completed to measure the difference between the speed of the vehicle's CG and the speed of the antenna when there is relative motion between the two. The VBOX antenna was mounted to the end of a swing arm of known length. The swing arm was actuated by a pneumatic cylinder. The swing arm was mounted in the bed of a truck so that its rotational axis was perpendicular to the vehicle path. The rotation angle and angular velocity of the swing arm

were measured with a string potentiometer and a rotational rate sensor. The test setup is shown in Figure 5. The truck was driven up to the desired test speed of approximately 40 mph, and the swing arm was actuated so that the arm rotated forward until it contacted the roof of the truck at an articulation angle of approximately 90°. The reference speed of the truck was measured using a Datron velocity sensor.

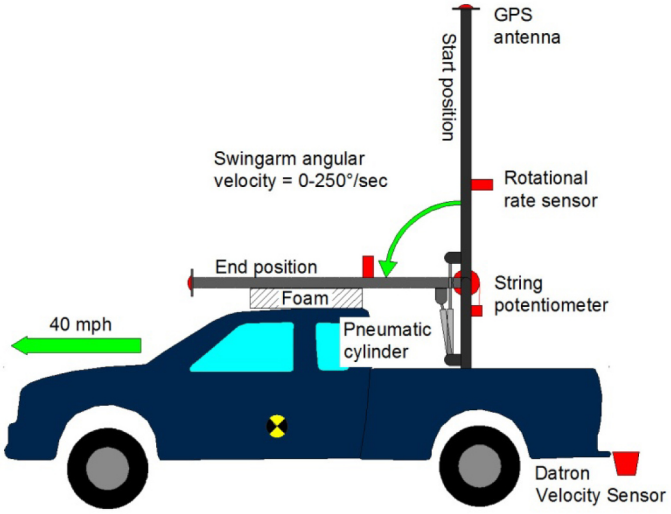

Figure 5. GPS speed sensor swing arm test setup.

DATA FILTERING

During the driving phase and the tripping phase, the vehicle is responding to the tire-to-ground forces, while during the rollover phase the vehicle is subjected to a series of short-duration impacts. Due to the dissimilarity in magnitude and duration of the forces applied before and after trip, two different levels of industry-standard filtering were applied to the acquired data. Prior to the trip point, the data was post-processed with a 6 Hz, 12-pole, phaseless filter, consistent with the protocol utilized by NHTSA in its NCAP fishhook testing [14]. After the trip point, the data acquired from the rollover phase was post-processed using a Class-60 filter, pursuant to SAE J211.

RESULTS

ROLLOVER TESTS

In the Appendix, the post-test photographs of the vehicles and test site are shown along with the reconstruction diagram and a summary of each test. Plots of the filtered data, including the acceleration traces (uncorrected) and the output of the VBOX speed sensor are also presented in the Appendix. In the data plots, time-zero is the synchronization trigger and the vertical line denotes the trip point.

The primary results of the rollover test analyses are presented in Table 2, Table 3, Table 4, Table 5.

Table 2. Roll path results.

	Roll Phase		Roll Distances			
Test	Rolls	Duration (sec)	Total (ft)	Longest (ft)	Shortest (ft)	Average (ft)
0	2.5	5.05	104.5	66.4	26.9	41.8
1	9	7.58	264.7	68.8	14.1	29.4
2	5	5.31	146.7	45.7	20.0	29.3
3	3.5	3.70	92.4	30.4	23.2	26.4
4	3	3.57	105.2	52.2	24.1	35.1

Table 3. First airborne phase results.

	Trip to First Ground Contact		
Test	OGS (mph)	Distance (ft)	Time (sec)
0	33.8	10.7	0.224
1	57.9	22.4	0.264
2	41.0	14.9	0.248
3	30.2	11.1	0.250
4	42.3	13.9	0.222

Table 4. Average drag factors for each test.

	Average Drag Factors		
Test	Total (g)	Intial (g)	Final (g)
0	0.36	0.51	0.25
1	0.42	0.66	0.21
2	0.38	0.53	0.35
3	0.33	0.62	0.26
4	0.57	0.71	0.42

Table 5. Orientation and roll rates at trip.

	Trip Orientation		Roll Rates*		
Test	Sideslip (deg)	Roll Angle (deg)	Trip (deg/s)	Peak (deg/s)	Average (deg/s)
0	35	65	234	383	178
1	28	69	268	760	427
2	51	57	347	591	339
3	68	54	342	532	341
4	26	75	171	421	302

****Rate sensor data not available for Test 4; results from OGS analysis.***

The OGS of each vehicle was plotted versus time to show the variation in deceleration (drag factor) throughout the rollover. This data is presented in Figure 6, Figure 7, Figure 8, Figure 9, Figure 10.

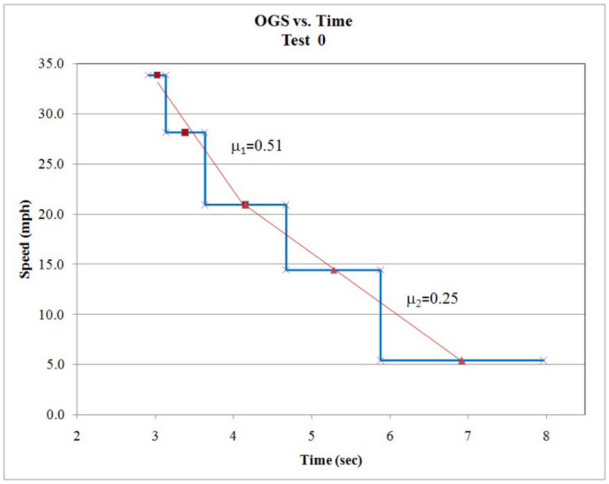

Figure 6. Plot of OGS vs. Time for Test 0.

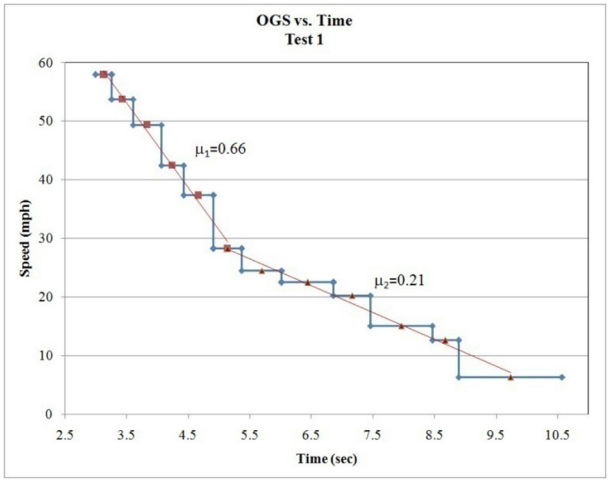

Figure 7. Plot of OGS vs. Time for Test 1.

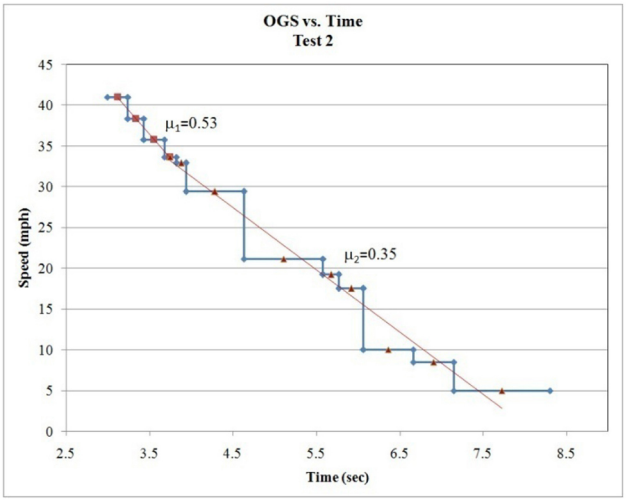

Figure 8. Plot of OGS vs. Time for Test 2.

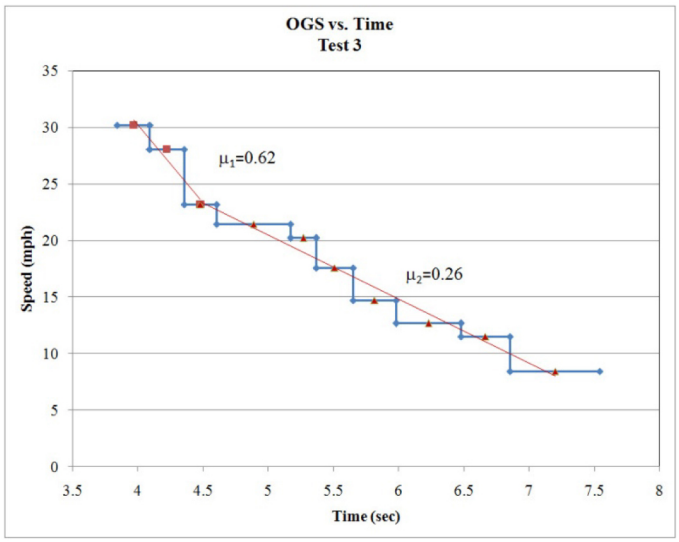

Figure 9. Plot of OGS vs. Time for Test 3.

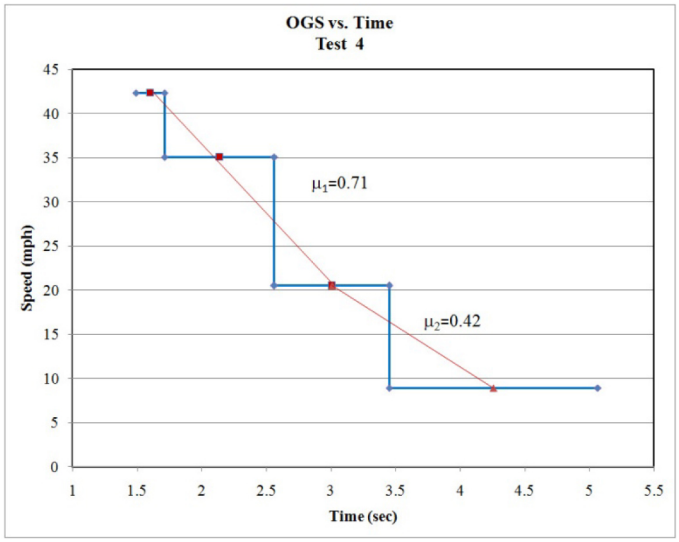

Figure 10. Plot of OGS vs. Time for Test 4.

GPS SPEED OUTPUT VERIFICATION TEST

The angular velocity of the swing arm went from 0°/sec at the start of the test to approximately 250°/sec at 75° of articulation. Results from three test runs reporting the error in speed versus articulation angle are shown in Figure 11. This chart demonstrates that the GPS reported speed exceeds the reference speed of the vehicle by more than 10% when the articulation angle exceeds 15°.

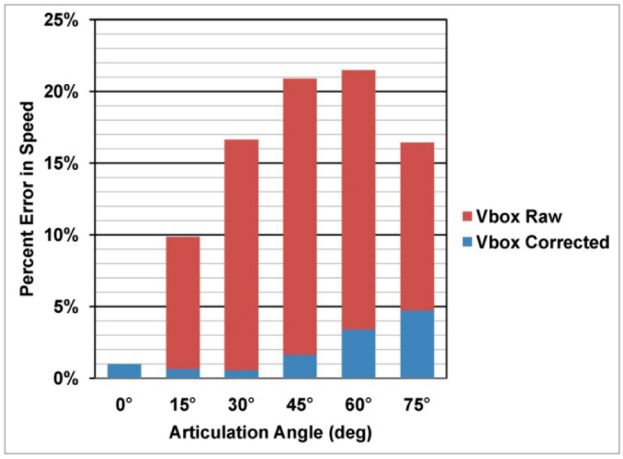

Figure 11. Swing arm test results.

TRIP POINT

In this study the trip point was defined as the termination of the leading tire marks (four-wheel lift). The instant of four-wheel lift was captured on multiple videos and was found to coincide with the measured accelerations dropping to zero and the termination of the tire marks.

In earlier works, the trip point has been defined as the instant when the vehicle's CG crosses the vertical plane between its leading tires. In all five tests reported here, the vehicle's CG crossed over the line of its leading tires at approximately 50° of roll, but the roll angle at four-wheel-lift was greater than 50° in each case. If the 50° roll condition had been used to define trip, the distance covered during the initial airborne phase of each test would have been over-reported by an average of 3.9 feet, indicating that the vehicle had tripped before the tire marks ended.

Another common definition for trip point is the time when the overturning vehicle's roll rate becomes constant. In Test 0, the roll rate peaked at the moment of four-wheel lift and then dropped to an approximately constant level during the remainder of the initial airborne phase. In Tests 1, 2, and 3, the roll rate increased up to the point of four-wheel lift and continued to rise for a short time, even after the vehicle was airborne. The roll rates then dropped to an approximately constant level until the first ground impact. The instrumentation failed to capture the roll rate of the vehicle during Test 4.

On average, the roll rate of the vehicles in the four tests for which accurate roll rate data was acquired did not reach a constant level until the vehicle had traveled an additional 3.9 feet through the air, past the end of its tire marks. Figures 12, 13, 14, 15 show the change in roll rate after the trip point in Tests 0, 1, 2, and 3, respectively.

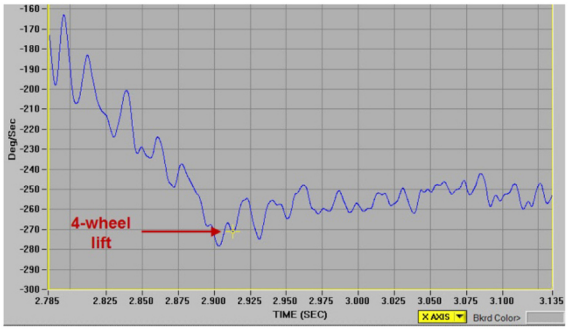

Figure 12. Roll rate at trip point in Test 0.

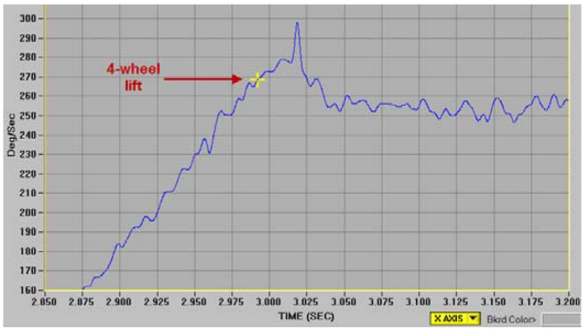

Figure 13. Roll rate at trip point in Test 1.

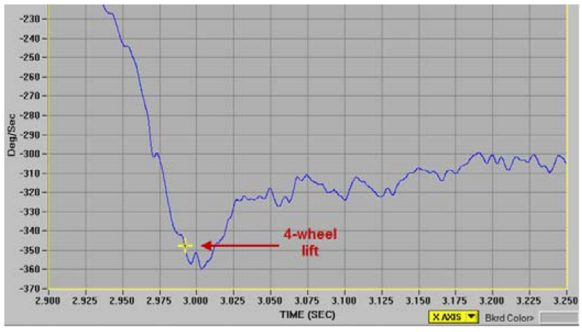

Figure 14. Roll rate at trip point in Test 2.

Figure 15. Roll rate at trip point in Test 3.

DISCUSSION

GPS SENSOR OUTPUT CORRECTION

During roll initiation, rotation occurs about the line between the tires on the leading side of the vehicle (Figure 16). The VBOX reports the antenna speed in the xy-plane which includes the xy-component of the tangential velocity of the antenna at any given time [15]. The time of interest for accident reconstruction is at the point of trip.

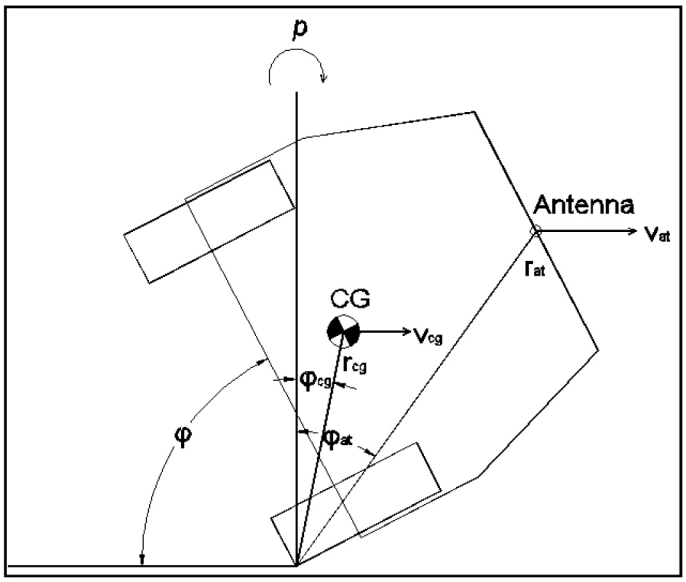

Figure 16. Vehicle parameters necessary to determine V_{cf} at point of trip.

The tangential velocity of the antenna is a function of the distance from the leading edge tires to the antenna (r_{at}), the roll velocity (p), and the roll angle (φ). It is further necessary to know the CG position in order to transform the speed of the antenna to the speed of the CG. A formula for the speed correction factor (V_{cf90}) when the vehicle's roll axis is perpendicular to the vehicle path, shown in Equation 2, can be derived from the above parameters. V_{cf90} is subtracted from the xy-component of the tangential velocity of the VBOX antenna to obtain the corrected speed of the CG.

$$V_{cf90} = r_{at} * p * \cos(\varphi_{at}) - r_{cg} * p * \cos(\varphi_{cg}) \quad (2)$$

This correction formula was applied to the VBOX speed output recorded in the verification tests. The results of this correction were presented in Figure 11. The corrected VBOX speed remains accurate up to a roll angle of 45° with an error of less than 2%. It is hypothesized that the decrease in corrected VBOX speed accuracy at roll angles in excess of 45° is related to an abrupt decrease in the number of satellites visible to the antenna and/or the inability of the device to discern what portion of its velocity is in the vertical direction due to the high roll angle. Figure 17 shows the speed signal and the number of satellites in Test 3, which starts with 12 visible satellites that begin to drop out as the vehicle approaches the trip point. Consistent with the other tests, the abrupt change in reported vehicle speed corresponds to the sudden loss in the number of visible satellites.

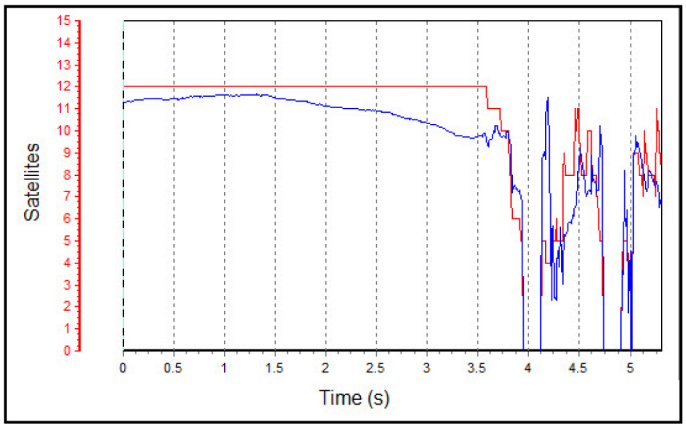

Figure 17. GPS speed signal and number of visible satellites for Test 3.

Rollover events seldom occur at a 90° slip angle. The vehicle slip angle will influence the GPS speed sensor correction because the tangential velocity of the VBOX antenna will not always be in line with the CG path, as shown in Figure 18. Therefore, it is necessary to know the slip angle at the point of trip. The error in the VBOX reported speed will be greatest when vehicle is at a ±90° slip angle (roll axis perpendicular to the vehicle path) and will diminish as the test vehicle's slip angle approaches 0° or 180° (roll axis parallel to the vehicle path).

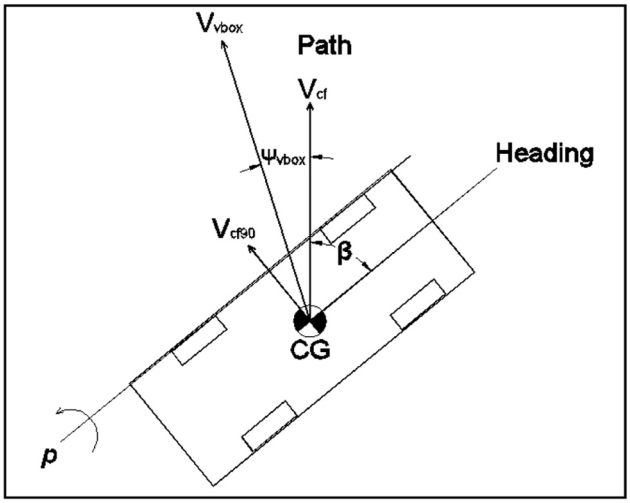

Figure 18. Slip angle influence on GPS speed sensor correction.

The vehicle slip angle (β) is the only additional information necessary to correct for this error. The formula utilized to perform this correction is presented as Equation 3. This formula was applied to Test 1 through Test 4 at the instant the roll angle was 45°. Forward integration of the acceleration data from the 45° roll point up to the point of trip was completed to estimate the trip speed from the data. The formula could not be applied to Test 0 due to the lack of the VBOX speed data.

$$V_{cf} = \sqrt{{V_{VBOX}}^2 + {V_{cf90}}^2 - 2 * V_{VBOX} * V_{cf90} * \cos(90 - \beta - \Psi_{VBOX})} \quad (3)$$

It is important to recognize that this correction is not specific to the GPS speed sensor used in these tests. It may generally be anticipated that during vehicle rotation, the measurement of acceleration, speed or displacement at a location away from the vehicle's CG would require some correction or transformation to estimate the same parameters at the vehicle's CG.

In rollovers, the application of a geometric correction, as described above, appears to have limited utility beyond roll angles of 45°. Therefore, correction of the GPS speed sensor to estimate the actual trip speed may still require integration of vehicle acceleration along its travel path from the position of 45° roll angle forward to the point of trip. Because all four test vehicles with VBOX data overturned at roll angles in excess of 45°, the GPS speed sensor geometric correction (Equation 3) could not fix the sensor errors at the trip points to determine the trip speeds. Instead, a two stage correction was applied. First, the VBOX speed output was corrected using Equation 3 at the point where each test vehicle had rolled to 45°. Then the measured accelerations (corrected for roll angle and sideslip) were integrated along the path to estimate the additional speed loss between the 45° position and the trip point. The roll rate sensor in Test 4 had a threshold of only 150 °/sec and became saturated when the vehicle had rolled only 31° so this became the starting point for the acceleration integration of that test.

The trip speeds calculated by this method are given in Table 6 along with the trip speeds reported by the GPS sensor. This correction lowered the VBOX reported speed by as much as 9.5 mph in Test 3, which resulted in a 32% error between the corrected speed and what was being reported by the sensor. The VBOX over-reported the speed by 2% to 32% for this set of rollover tests.

Table 6. VBOX reported and corrected trip speeds.

Test	VBOX Trip Speed		
	Reported (mph)	Corrected (mph)	% Error
1	64.6	60.6	7
2	45.2	39.4	15
3	39.0	29.5	32
4	47.1	46.2	2

When compared to the trip speed from the OGS analysis, the difference in the VBOX corrected speed (VBOX-C) was within 3% to 8%, as shown in Table 7. The test with the greatest error between the corrected speed and the OGS was Test 4. In this test, the only acceleration data acquired was that from the VBOX Inertial Measurement Unit (IMU) which has a limited range and sampled at 100 Hz. This is believed to be a source of the larger correction error in Test 4. This correction procedure proved to be an appropriate adjustment at the point of trip in these rollover tests.

Table 7. Comparison of OGS speed and VBOX corrected speed.

Test	Trip Speed Comparison		
	OGS (mph)	VBOX-C (mph)	% Error
1	57.9	60.6	4
2	41.0	39.4	4
3	30.2	29.5	3
4	42.3	46.2	8

For Test 0, no data was recorded by the GPS speed sensor. The speed of the vehicle at the start of data acquisition was determined by video analysis and survey data of the site and tire marks. The speed at overturn was determined by calculating the component of the X, Y, and Z acceleration data along the vehicle's path and integrating the path acceleration up to the point of trip. The trip speed calculated by the OGS analysis of Test 0 agreed with the integrated acceleration result to within 1 mph, a difference of less than 3%.

AVERAGE DRAG FACTORS

The average drag factor for each test was calculated based on the OGS analysis. The results, shown in Table 4, range from 0.33-0.57g. The mean drag factor of the five tests was 0.41g. These results are within the range of previously published values for dolly rollover tests and steer-induced roll tests.

In two of the tests reported here, the vehicles tripped and rolled on the asphalt roadway before rolling to rest off-road,

resulting in drag factors of 0.38g and 0.42g. In one of the tests, the vehicle tripped and rolled entirely on the concrete pavement, which resulted in a drag factor of 0.36g. The other two test vehicles tripped and rolled in desert soil, producing drag factors of 0.33g and 0.57g. Within this series of rollovers, there does not appear to be a correlation between the drag factors and the roll surfaces.

BILINEAR DECELERATIONS AND ROLL RATE PEAK

The plots of the OGS vs. Time indicate a variable deceleration of the vehicles during the rollover. All of the tests had a greater slope in the early part of the roll phase than in the latter part. This concept of a variable deceleration has been discussed in prior works by Carter [11] and by Rose and Beauchamp [12].

When evaluating the test data, one obvious challenge is to determine the best manner to represent the deceleration trend. In each test, a knee in the OGS vs. time curve was observed at which the deceleration rate appeared to decrease. The data before and after the knee in the curve were well fit by linear approximations. The drag factor before and after the change in deceleration rate are equal to the slopes of the two linear approximations to the OGS vs. Time curve for each test, as shown in Figure 6, Figure 7, Figure 8, Figure 9, Figure 10.

The initial drag factors for each test ranged from 0.51 - 0.71g while the final drag factors had a range of 0.21 - 0.42g. Table 4 presents the initial and final drag factors for each test.

By comparing the time histories of the OGS for Tests 1, 2, and 3 (Figure 7, Figure 8, Figure 9) and the roll rates (shown in the Appendix), it was observed that the change in drag factor and the peak roll rate occurred at similar points in time.

TRIP POINT

The way in which the trip point of a test is defined can have a significant effect on the measured duration and distance of the first airborne phase. The continued rise in roll rate after the point of four-wheel lift (the end of external roadway forces on the vehicle) may be due to a change in the roll inertia of the vehicle once it is airborne. It may be that the unsprung mass of the vehicle (axles, wheels, driveline, etc.) moves relative to the rest of the vehicle after the tire forces are removed, changing the roll inertia and affecting the roll rate.

OBSERVATIONS

• The average distance per roll for each test (as shown in Table 2) ranged from 26.4 to 41.8 feet.

• The shortest roll distance in Test 1 was just over 14 feet (Table 2), with the vehicle completing an airborne roll in a distance that was less than its circumference. This occurred during roll number 6 of the 9-roll test.

• The duration of the first airborne phase in all five tests was between 0.22 to 0.26 seconds. Despite significant variations in speed, sideslip, roll rate, and ground surface at the point of trip, the duration of the first airborne phases did not vary by more than 0.04 seconds.

• The tests with the greatest roll angles at trip also had the lowest sideslip angles (see Table 5). In Test 4, with a sideslip of only 28°, the vehicle rolled to 75° before its tires lost contact with the ground. In contrast, the vehicle in Test 3 experienced four-wheel lift at a roll angle of only 54° but a sideslip of 68°.

• The average drag factors over the rollover phase, which were calculated from the OGS analysis, ranged from 0.33 - 0.57g, with a mean of 0.41g.

• The rollover surface does not appear to have a noticeable effect on the average drag factor in these five tests.

• For all five tests reported here, the point of four-wheel lift (trip point) in each test occurred after the CG had passed over the leading tires and before the roll rate became constant.

• Approximating the vehicle's trip point as the moment that the CG crosses the vertical plane of its leading tires would have resulted in an overstatement of the distance from trip to first ground contact in these tests.

• For the four tests in which accurate roll rate data was acquired, the point of four-wheel lift occurred before the roll rate became constant.

• Approximating the trip point as the instant when the vehicle's roll rate becomes constant would have understated the length of the first airborne phase.

• Comparing the rate of change in the OGS and the roll rate data for Tests 1, 2, and 3, it was observed that the reduction in drag factor and the peak roll rate occurred at similar points in time.

CONCLUSIONS

• Analysis of onboard instrumentation data, multi-angle video coverage, and survey data combined with detailed vehicle inspections proved to be an accurate method for reconstructing the vehicle OGS throughout a rollover test.

• The ability to synchronize the test instrument data, video footage, and survey data using flashbulbs and a chalk gun proved to be a key factor in this type of vehicle testing.

• In rollover testing, a roof-mounted GPS speed sensor will overestimate the speed of the vehicle due to the rotational speed component of the sensor antenna relative to the vehicle CG.

• A correction factor was proposed to adjust the GPS speed sensor data when used in rollover testing. For the tests performed in this work, it was additionally necessary to use integration of the accelerometer data in conjunction with this correction factor when the vehicle reached a roll angle in excess of 45°.

• The OGS speed curve for each test was well approximated with a bilinear fit. The slopes of the two trend-lines represent the initial and final drag factors of the roll event.

CONTACT INFORMATION

Don C. Stevens
123. S. Weber Drive
Chandler, AZ 85226
(480) 706-2963
don@sefainc.com

ACKNOWLEDGMENTS

The Authors wish to acknowledge the significant contribution of Michael Rosenfield, RSR Engineering, LLC. The contribution of time, insight, and expertise provided by Mr. Rosenfield in the execution of the testing presented in this paper was invaluable and made significant impact upon its successful completion. The Authors also wish to thank the Southwest Association of Technical Accident Investigators for allowing us the use of their robotic steering system.

REFERENCES

1. Yaek, J.L., Curry, B., and Goertz, A., "Review and Comparison of Published Rollover Test Results," SAE Technical Paper 2010-01-0057, 2010, doi: 10.4271/2010-01-0057.

2. Asay, A.F. and Woolley, R.L., "Rollover Testing on an Actual Highway," SAE Technical Paper 2009-01-1544, 2009, doi:10.4271/2009-01-1544.

3. Larson, R.E., Smith, J.W., Werner, S.M., and Fowler, G.F., "Vehicle Rollover Testing, Methodologies in Recreating Rollover Collisions," SAE Technical Paper 2000-01-1641, 2000, doi:10.4271/2000-01-1641.

4. Wilson, L. A., Gilbert, M., Godrick, D. A., "Reconstruction and Analysis of Steering-Induced On-Road Untripped SUV Rollover Test (Part 2)," Collision: The International Compendium for Crash Research 2(2):124-129, 2007.

5. Asay, A.F. and Woolley, R.L., "Rollover Testing of Sport Utility Vehicles (SUVs) on an Actual Highway," SAE Technical Paper 2010-01-0521, 2010, doi: 10.4271/2010-01-0521.

6. Hight, P.V., Siegel, A.W., and Nahum, A.M., "Injury Mechanism in Rollover Collisions," SAE Technical Paper 720966, 1972, doi: 10.4271/720966.

7. Orlowski, K.F., Moffatt, E.A., Bundorf, R.T., and Holcomb, M.P., "Reconstruction of Rollover Collisions," SAE Technical Paper 890857, 1989, doi: 10.4271/890857.

8. Martinez, J.E. and Shlueter, R.J., "A Primer on the Reconstruction and Presentation of Rollover Accidents," SAE Technical Paper 960647, 1996, doi:10.4271/96-647.

9. Meyer, S.E., Davis, M., Forrest, S., Chng, D. et al., "Accident Reconstruction of Rollover - A Methodology," SAE Technical Paper 2000-01-0853, 2000, doi: 10.4271/2000-01-0853.

10. Luepke, P.A., Carter, J.W., Henry, K.C., Germane, G.J. et al, "Rollover Crash Tests on Dirt: An Examination of Rollover Dynamics," SAE Technical Paper 2008-01-0156, 2008, doi:10.4271/2008-01-0156.

11. Carter, J.W., Luepke, P., Henry, K.C., Germane, G.J. et al., "Rollover Dynamics: An Exploration of the Fundamentals," SAE Technical Paper 2008-01-0172, 2008, doi:10.4271/2008-01-0172.

12. Rose, N.A. and Beauchamp, G., "Development of a Variable Deceleration Rate Approach to Rollover Crash Reconstruction," SAE Technical Paper 2009-01-0093, 2009, doi:10.4271/2009-01-0093.

13. Anderson, J.D., Gee, R.S., Germane, G.J., Henry, K.C. et al., "Analysis of a Real-World High-Speed Rollover Crash from a Video Record and Physical Evidence," SAE Technical Paper 2008-01-1486, 2008, doi:10.4271/2008-01-1486.

14. Forkenbrock, G. J., "A Demonstration of the Dynamic Tests Developed for NHTSA's NCAP Rollover Rating System - Phase VIII of NHTSA's Light Vehicle Rollover Research Program," DOT HS 809 705, 19, August 2004.

15. Customer Support Technician, VBOX USA, personal communication, June 2010.

APPENDIX A

TEST DATA

Test 0 Photos and Video Captures










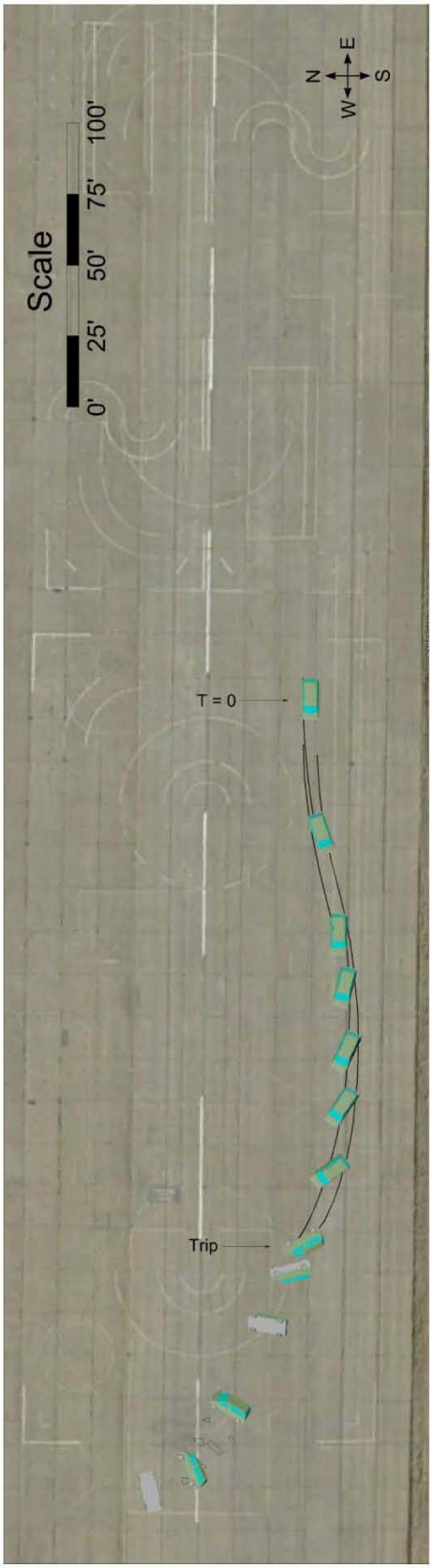

Test 0

Test #0 Notes
• 1989 Ford Aerostar XL 4x2
• Vehicle Test Weight: 4180 lbs
• Tires: Firestone FR380 P215/70R14 M+S
• Tire pressure: Pre-test: LF = 32 psi, RF = 32 psi, LR = 35.5 psi, RR = 35 psi Post-test: LF = 35.5 psi, RF = 34.5 psi, LR = 38.5psi, RR = 38 psi
• Driver side leading rollover
• Trip surface: Concrete
• Roll surface: Concrete
• Ambient temperature 97 °F
• No VBOX data recorded
• No string pots on wheels
• One flashbulb used instead of two

1989 Ford Aerostar **2.5 Rolls** **Test #0**

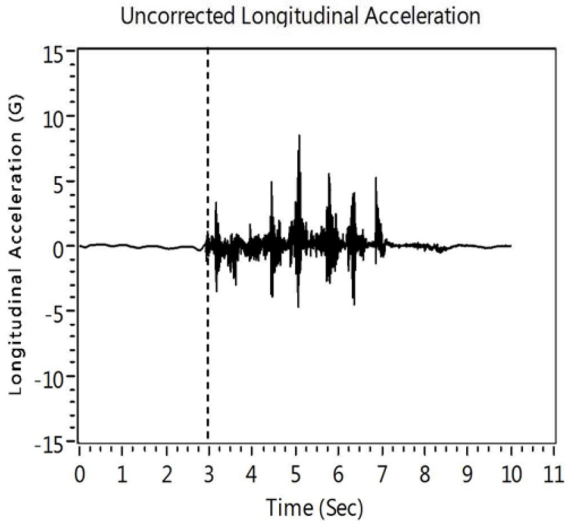

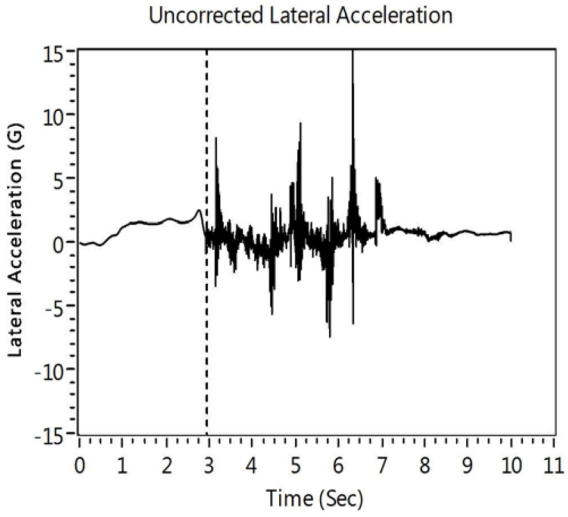

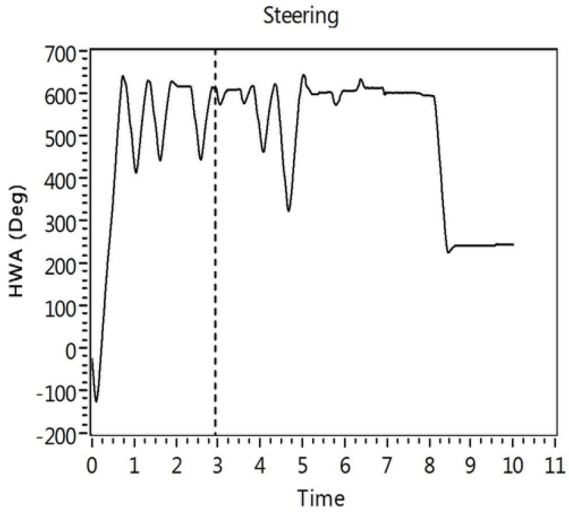

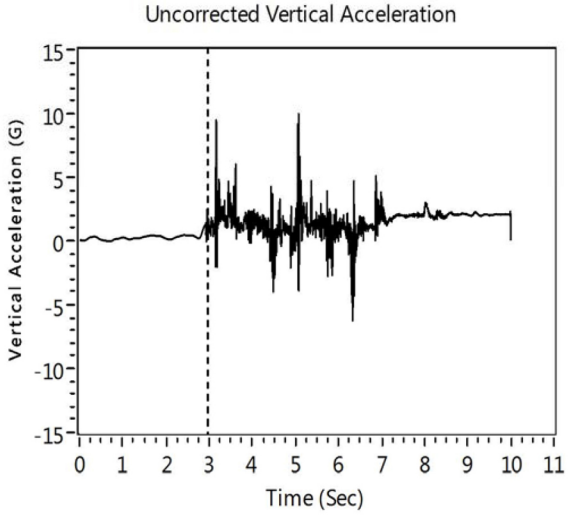

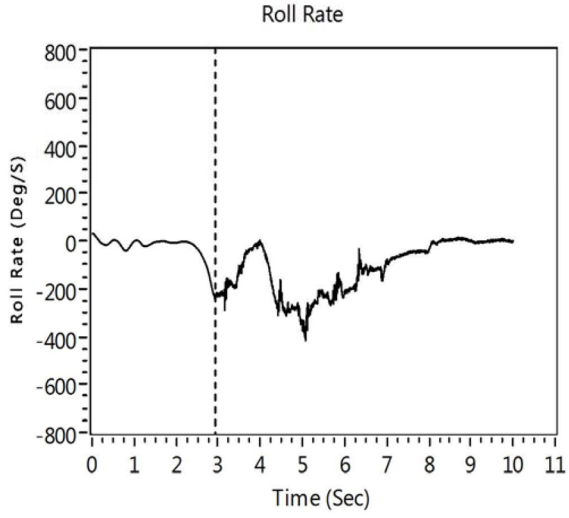

All data filtered 6Hz prior to trip point, class 60 after trip point; HWA unfiltered

Test 1 Photos and Video Captures










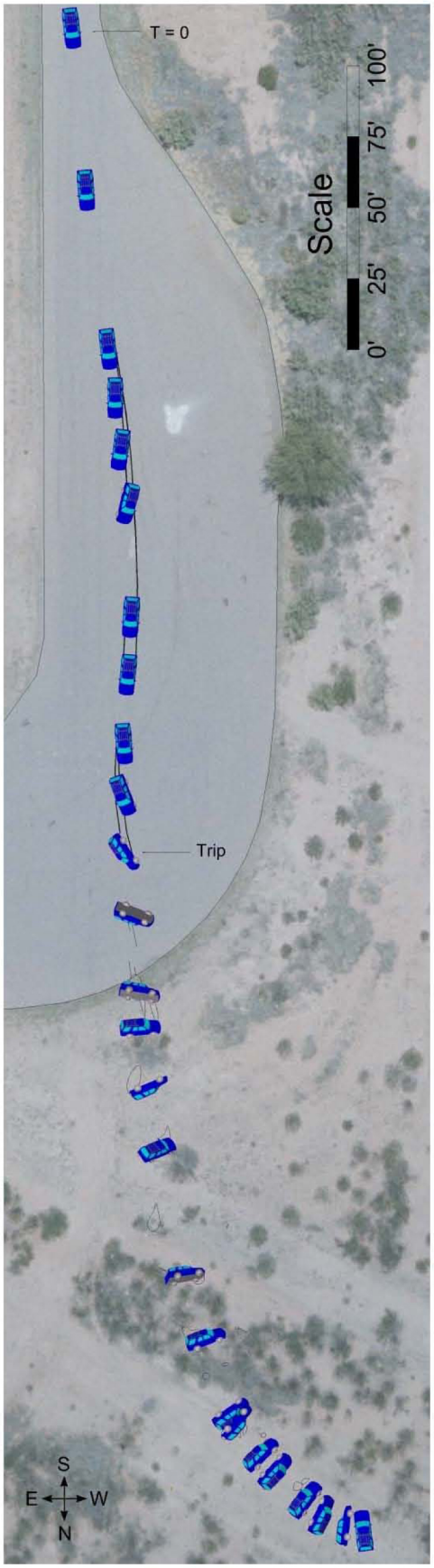

Test 1

Test #1 Notes
• 2001 Chevrolet Blazer 2DR 4x2
• Vehicle Test Weight: 4485 lbs
• Tires: Uniroyal Laredo P235/70R15
• Tire pressure: Pre-test: All four tires 32 psi Post-test: LR = 30.5 psi, LF/RF/RR = 0 psi
• Passenger side leading rollover
• Trip surface: Asphalt
• Roll surface: Asphalt for first 3/4 roll, then desert soil
• Ambient temperature 50 °F, rainfall previous day
• Tipped up on driver side tires then came back down before tipping up on passenger side tires

2001 Chevrolet Blazer **9 Rolls** **Test #1**

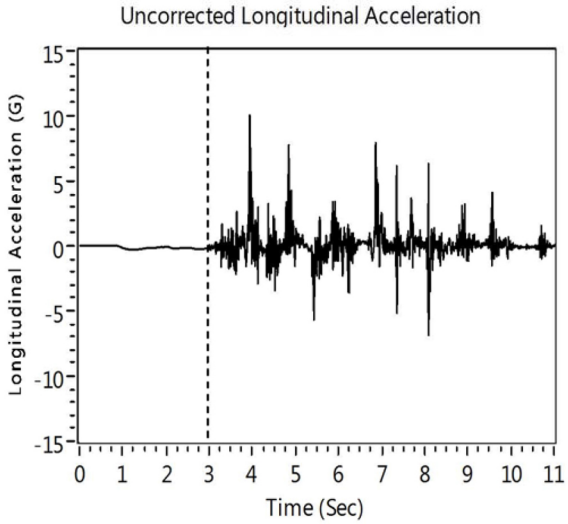

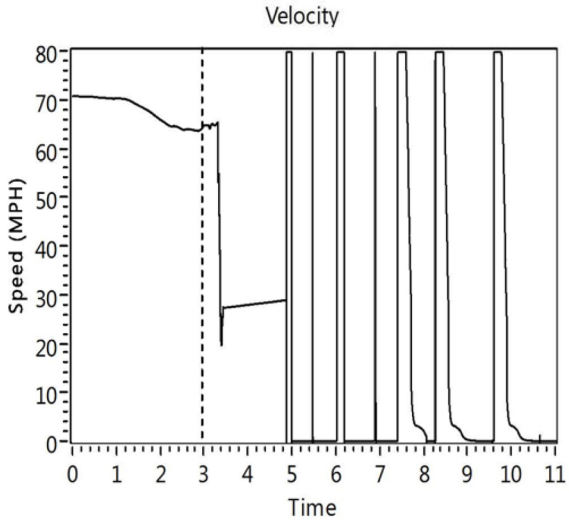

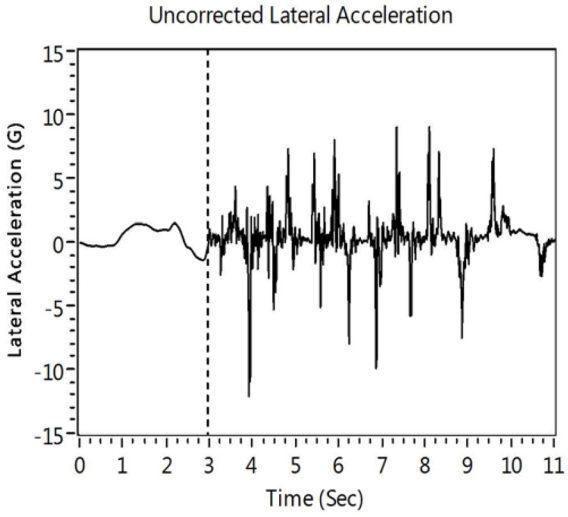

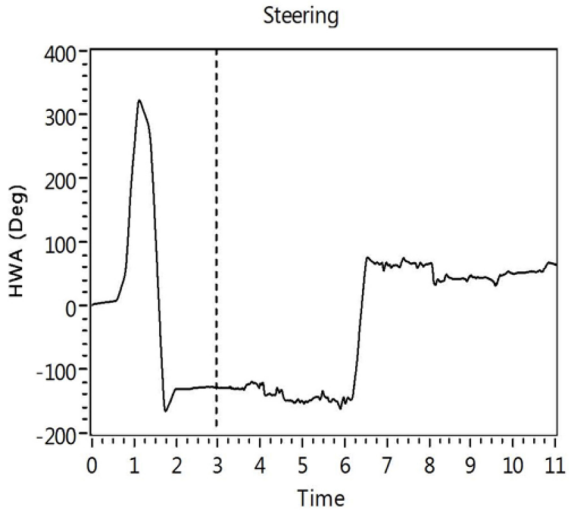

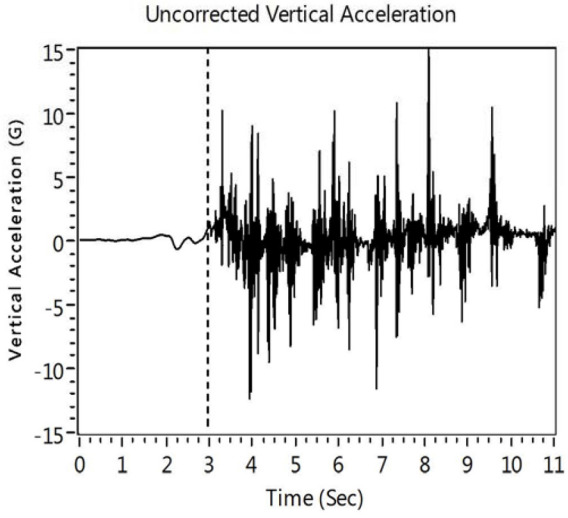

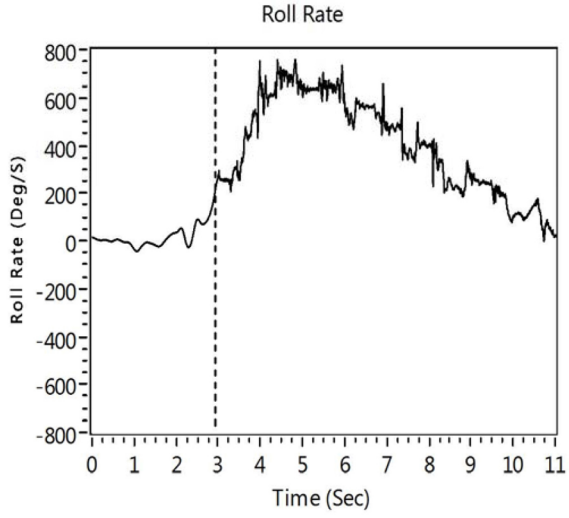

All data filtered 6Hz phaseless filter prior to trip point, class 60 phaseless filter after trip point; Speed and HWA unfiltered

Test 2 Photos and Video Captures

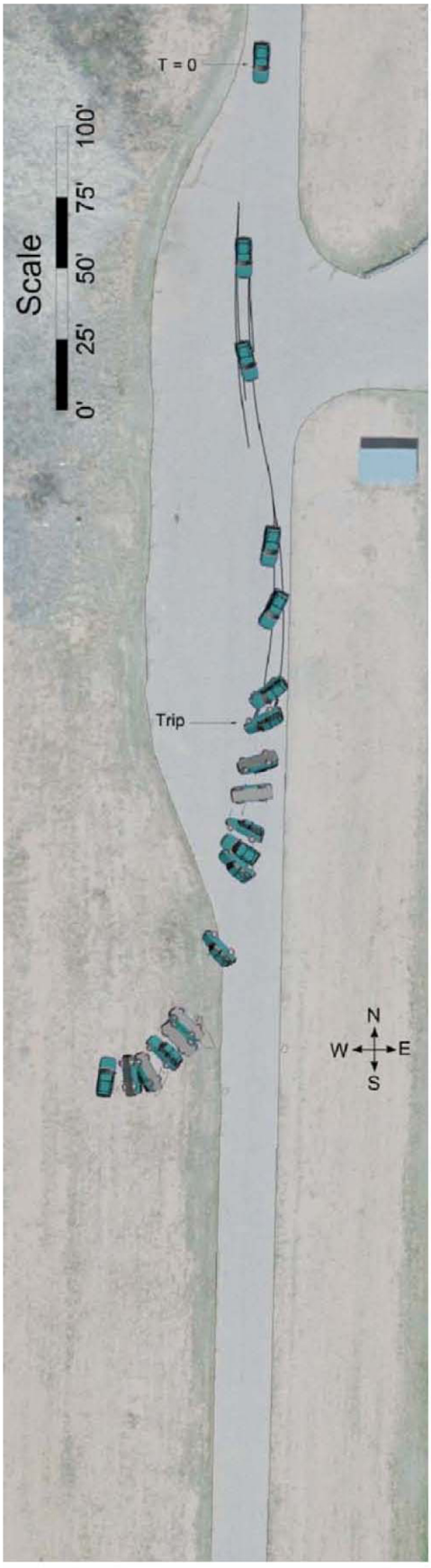

Test 2

Test #2 Notes
• 2002 Ford Explorer Sport 4x2 • Vehicle Test Weight: 4825 lbs • Tires: Continental Contitrac P235/70R16 M+S • Tire pressure: Pre-test: 30 psi front, 35 psi rear • Driver side leading rollover • Trip surface: Asphalt • Roll surface: Asphalt for first 2 rolls, then desert soil • Ambient temperature 50 °F, light rainfall previous day • VBOX IMU present

2002 Ford Explorer Sport **5 Rolls** **Test #2**

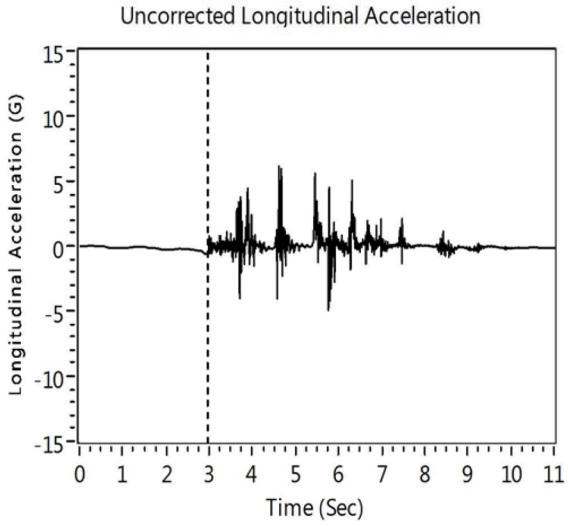

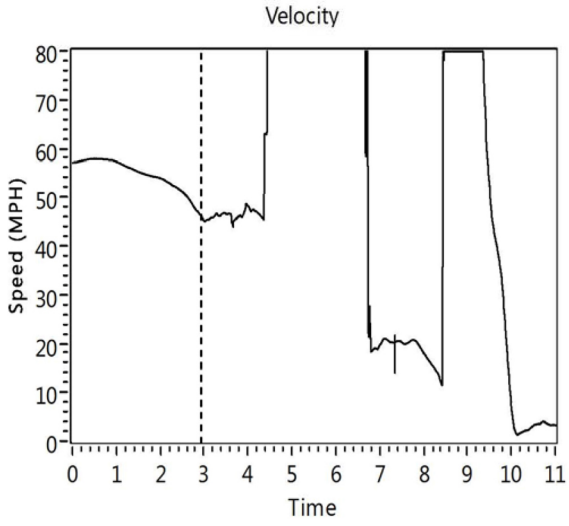

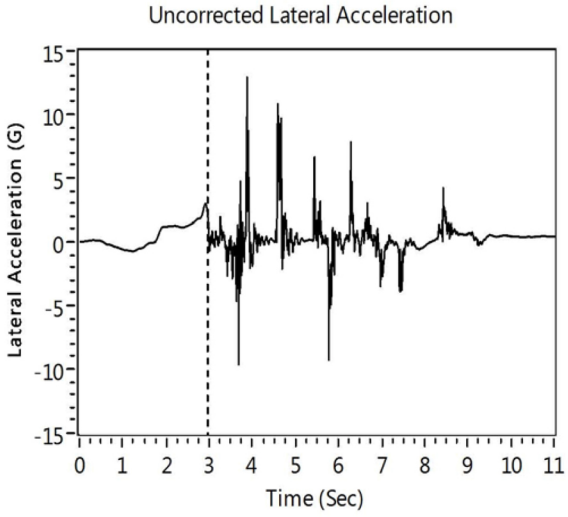

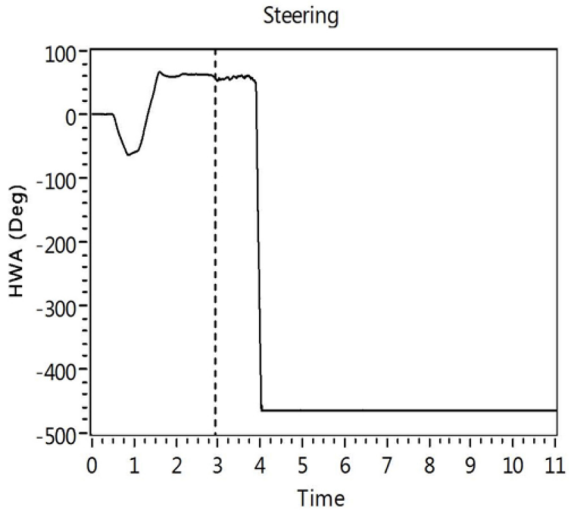

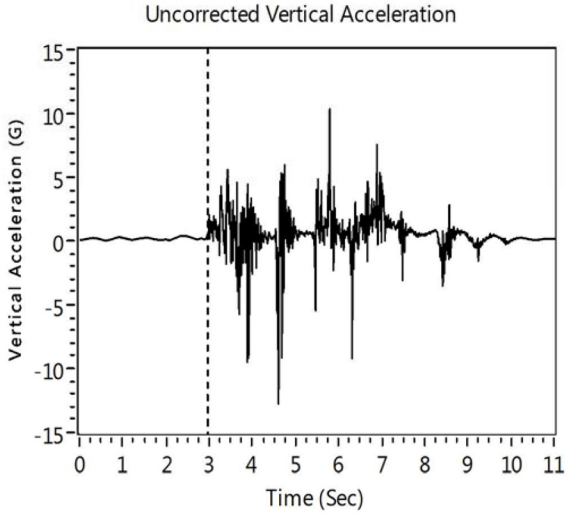

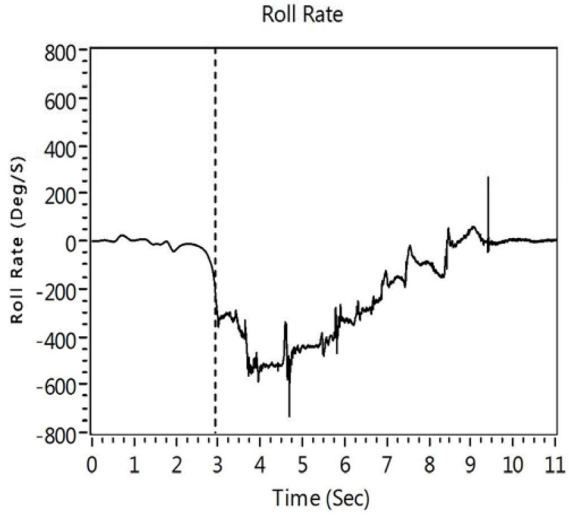

All data filtered 6Hz phaseless filter prior to trip point, class 60 phaseless filter after trip point; Speed and HWA unfiltered

Test 3 Photos and Video Captures










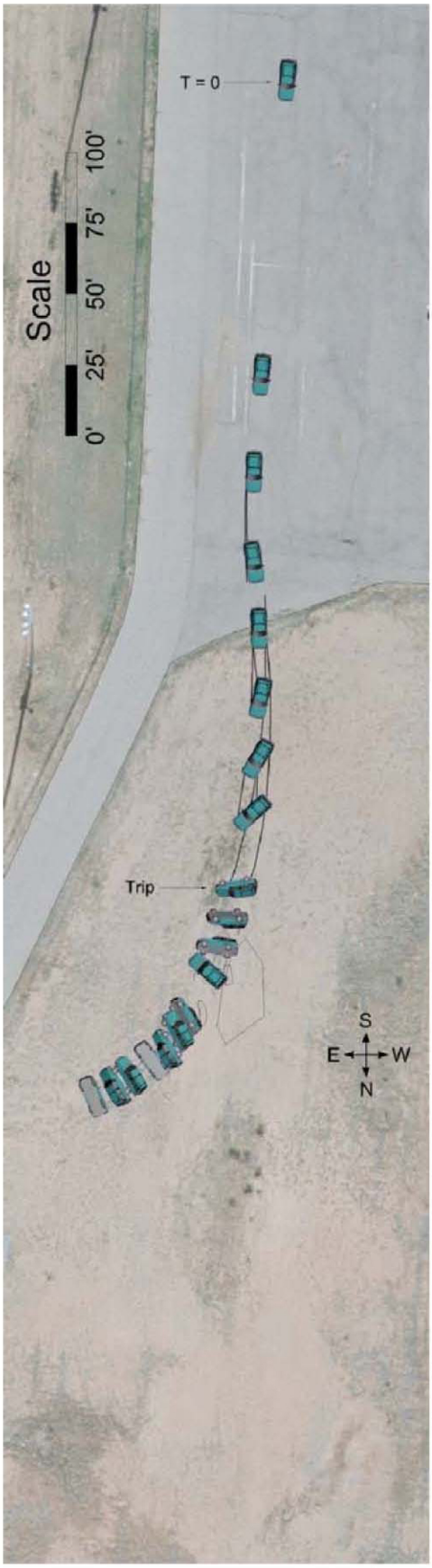

Test 3

Test #3 Notes
• 1997 Ford Explorer Sport 4x4
• Vehicle Test Weight: 5025 lbs
• Tires: Avon Radial SXT All Terrain 30x9.50R15LT
• Tire pressure:
Pre-test: All four tires 36 psi
Post-test: RF = 31 psi, RR = 24.5 psi, LF/LR = 0 psi
• Driver side leading rollover
• Trip surface: Desert soil
• Roll surface: Desert soil
• Ambient temperature 75 °F
• LF tire debeads approaching trip
• Dust cloud obstructs video footage for first 1.5 rolls

1997 Ford Explorer Sport **3.5 Rolls** **Test #3**

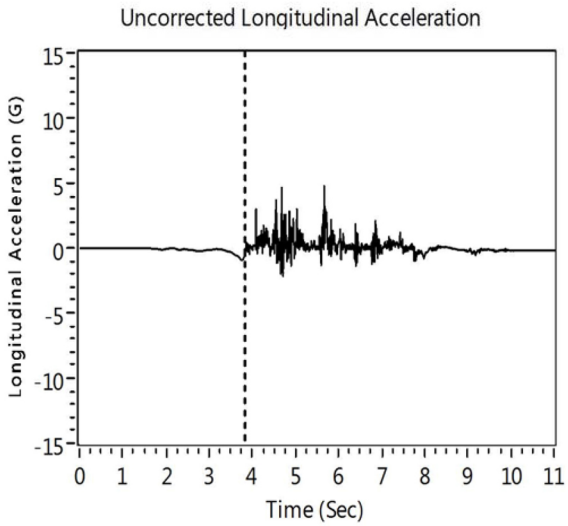

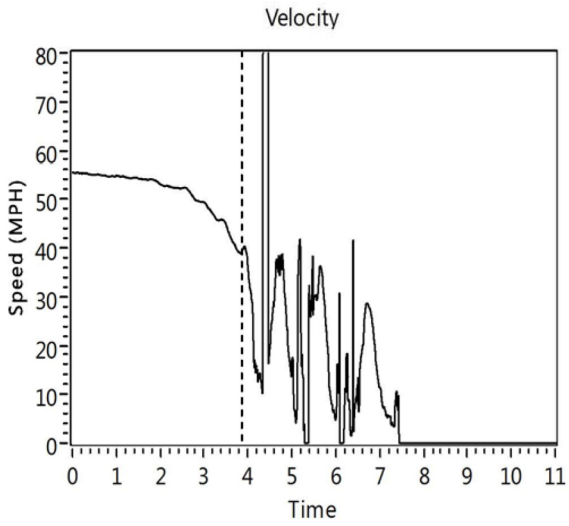

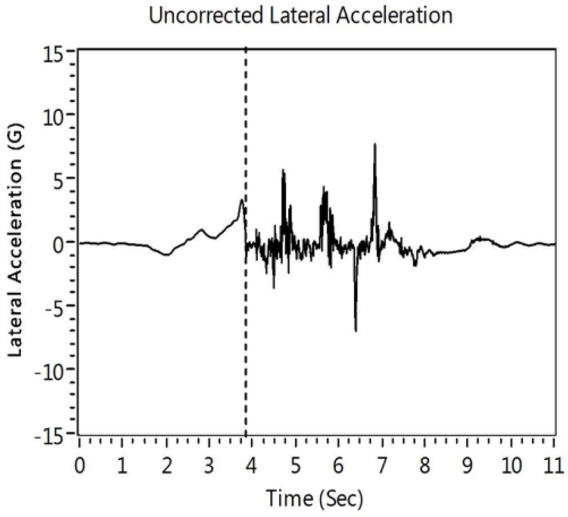

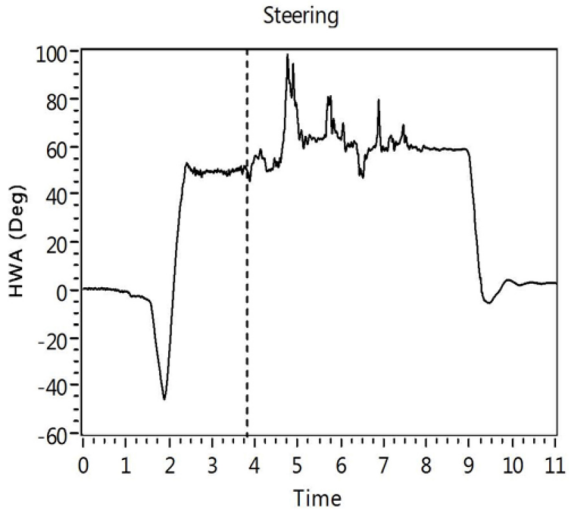

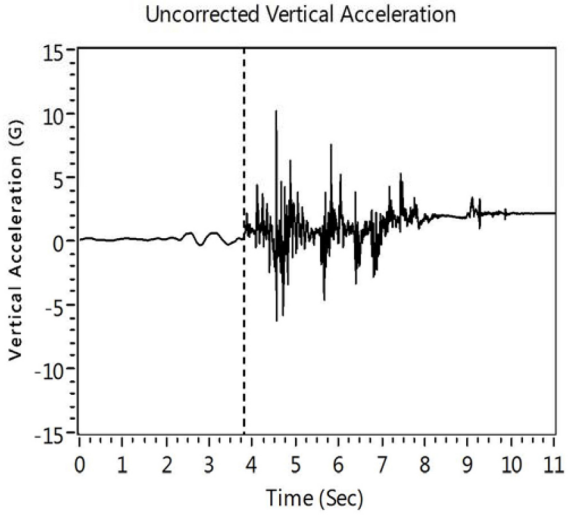

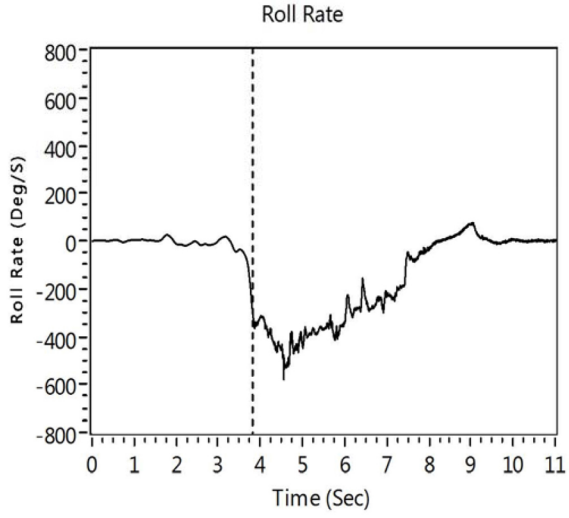

All data filtered 6Hz phaseless filter prior to trip point, class 60 phaseless filter after trip point; Speed and HWA unfiltered

Test 4 Photos and Video Captures

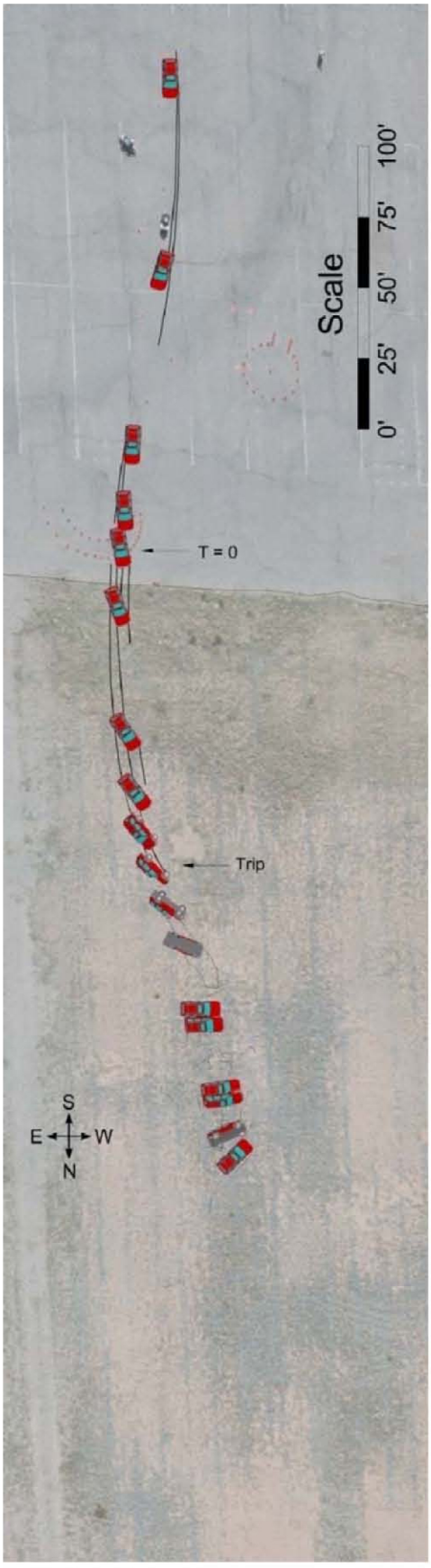

Test 4

Test #4 Notes
• 1995 Nissan Pathfinder LE 4x4
• Vehicle Test Weight: 4476 lbs
• Tire s: Dunlop A/T Radial Rover P235/75R15 M+S
• Tire pressure: Pre-test: All four tires 27.5 psi Post-test: LF/LR = 29 psi, RF/RR = 0 psi
• Passenger side leading rollover
• Trip surface: Desert soil
• Roll surface: Desert soil
• Soil was wet with a watering truck about 1 hour prior to test
• Ambient temperature 105 °F, winds up to 30 mph
• VBOX IMU present, but range is limited
• TDAS data collection failure
• Late trigger time
• RF tire debeads approaching trip
• Minimum ground clearance during vault phase
• Vehicle impacted field camera
• Spare tire carrier swung open at beginning of second roll
• Hood opened and swung off during last roll

1995 Pathfinder **3 Rolls** **Test #4**

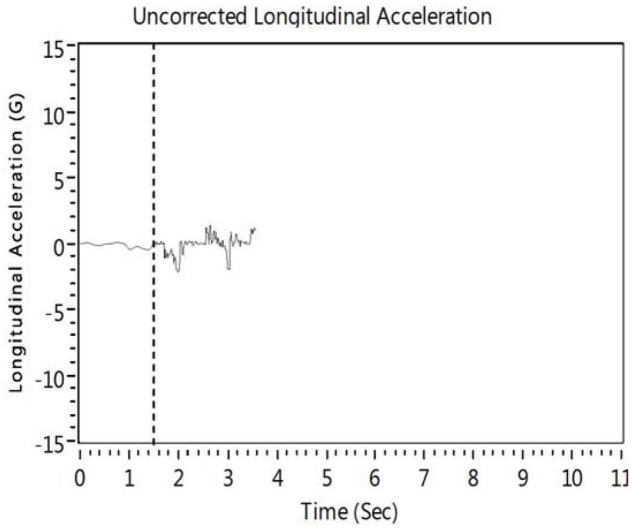

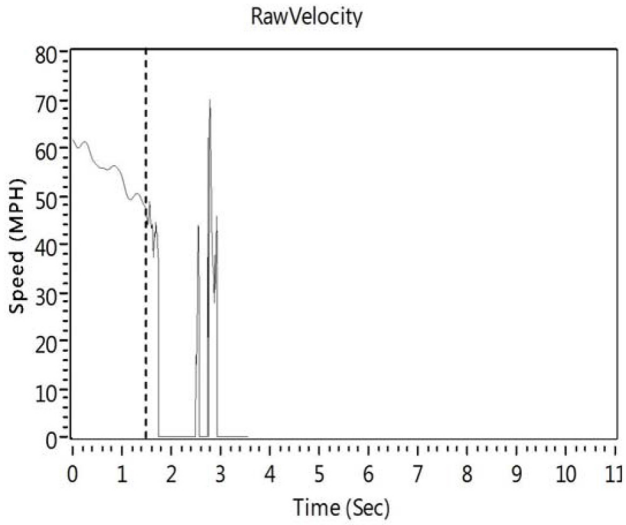

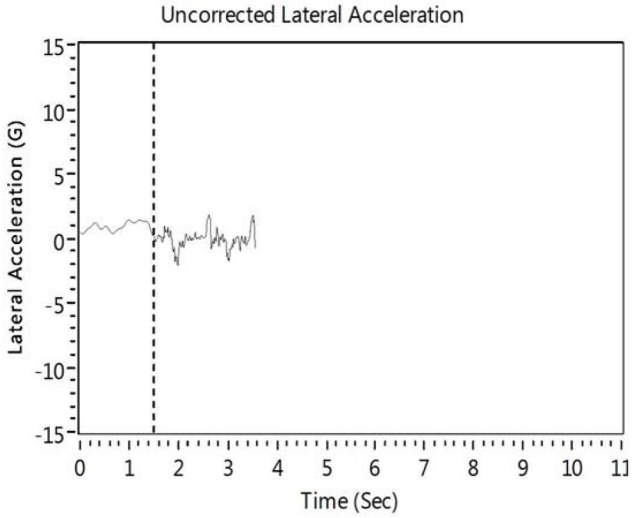

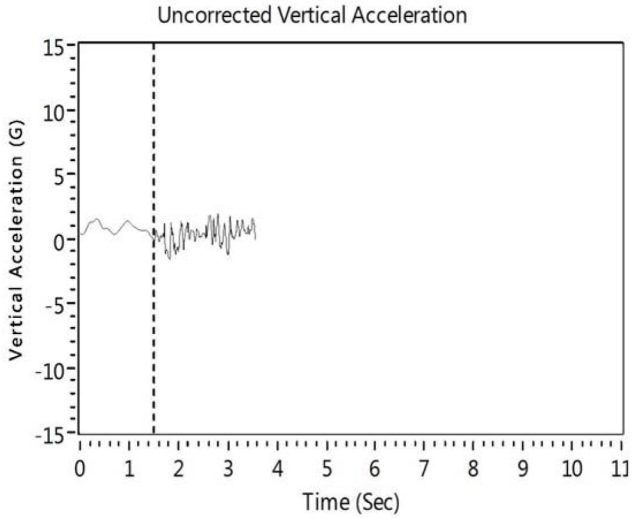

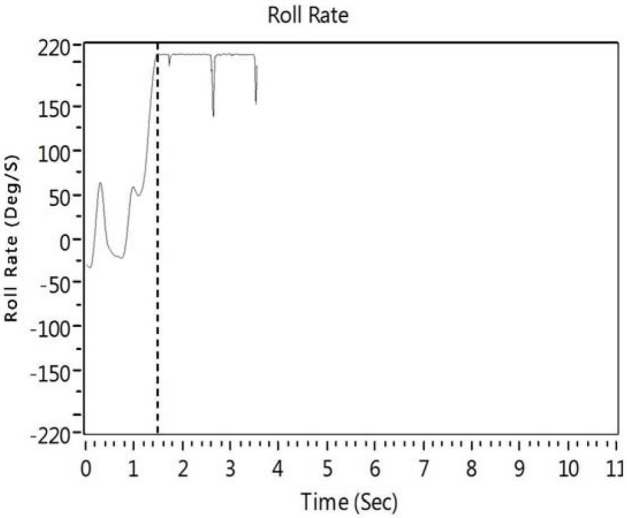

All data filtered 6Hz phaseless filter prior to trip point, class 60 phaseless filter after trip point; Speed and HWA unfiltered

ISSN 0148-7191

SAE Customer Service:
Tel: 877-606-7323 (inside USA and Canada)
Tel: 724-776-4970 (outside USA)
Fax: 724-776-0790
Email: CustomerService@sae.org
SAE Web Address: http://www.sae.org
Printed in USA